Available online at www.sciencedirect.com
ScienceDirect
Cancer Letters 271 (2008) 47–55
CANCER Letters
www.elsevier.com/locate/canlet

Mechanism of anticancer activity of buforin IIb, a histone H2A-derived peptide

Hyun Soo Lee [a,1], Chan Bae Park [a,1], Jung Min Kim [a], Su A Jang [a], In Yup Park [a], Mi Sun Kim [b], Ju Hyun Cho [c,*], Sun Chang Kim [a,*]

[a] *Department of Biological Sciences, Korea Advanced Institute of Science and Technology, Daejeon 305-701, South Korea*
[b] *Biomass Team, Korea Institute of Energy Research, Daejeon 305-343, South Korea*
[c] *Department of Biology, Research Institute of Life Science, Gyeongsang National University, Jinju 660-701, South Korea*

Received 2 February 2008; received in revised form 16 May 2008; accepted 23 May 2008

Abstract

Buforin IIb is a novel cell-penetrating anticancer peptide derived from histone H2A. Here we analyzed the anticancer activity and cancer cell-killing mechanism of buforin IIb. Buforin IIb displayed selective cytotoxicity against 62 cancer cell lines by specifically targeting cancer cells through interaction with cell surface gangliosides. It traversed cancer cell membranes without damaging them and accumulated primarily in the nuclei. Once inside the cells, buforin IIb induced mitochondria-dependent apoptosis. *In vivo* analysis revealed that buforin IIb displayed significant tumor suppression activity in mice with tumor xenograft. Overall, these results suggest that buforin IIb constitutes a novel therapeutic agent for the treatment of cancers.

Keywords: Anticancer peptide; Buforin IIb; Ganglioside; Histone H2A

1. Introduction

Numerous chemotherapeutic drugs have been developed to treat cancers, including DNA-alkylating agents, antimetabolites, and hormone agonists/antagonists. Although these drugs have been successfully used for the treatment of metastatic cancers, severe side-effects and dose limitations are prevalent. As a result of their inability to distinguish between cancer cells and proliferating normal cells, current drugs kill both. Moreover, cancer cells develop resistance to these drugs that is mediated by the overexpression of multidrug-resistance proteins that pump the drugs out of cells and thus render the drugs ineffective [1]. To overcome the limits of current chemotherapeutic drugs, many researchers have labored to identify new anticancer molecules. Recently, anticancer peptides have received attention as alternative chemotherapeutic agents that overcome the limits of current drugs. These peptides have sev-

* Corresponding authors. Tel.: +82 42 869 2619; fax: +82 42 869 2610 (S.C.Kim); Tel.: +82 55 751 5950; fax: +82 55 754 0086 (J.H.Cho).
E-mail addresses: juhyun.cho@gnu.ac.kr (J.H. Cho), sunkim@kaist.ac.kr (S.C. Kim).
[1] These authors contributed equally to this work.

0304-3835/$ - see front matter © 2008 Elsevier Ireland Ltd. All rights reserved.
doi:10.1016/j.canlet.2008.05.041

eral advantages over currently used anticancer therapeutics, such as selective cytotoxicity for cancer cells, bypass of the multidrug-resistance mechanism, and additive effects in combination therapy [2].

Several cationic antimicrobial peptides (AMPs) display anticancer activity. One such peptide, melittin, specifically counterselects for cells in culture that express high levels of the ras oncogene [3]. Cecropins and magainins also kill neoplastic cells at concentrations lower than those required to lyse normal cells such as peripheral blood lymphocytes [4,5]. Although some researchers have suggested that these peptides exert cytolytic activity against cancer cells through ion-permeable channel formation in the cell membrane [5], the precise mechanism of the cancer cell-killing action of the peptides remains to be deciphered. Despite the physicochemical properties it shares with other α-helical peptides [6], buforin II, an AMP with a helix–hinge–helix structure derived from histone H2A, has a unique mechanism of action: It rapidly crosses bacterial membranes without lysing cells; rather, it kills bacteria by interacting with intracellular macromolecules [7]. Buforin IIb is a synthetic analog of buforin II that contains a proline hinge in the middle and a model α-helical sequence at C-terminus (3×RLLR) [8]. Preliminary study showed that the hybrid peptide buforin IIb had stronger cytolytic activity against cancer cells than buforin II. Therefore, here we analyzed the anticancer activity and cancer cell-killing mechanism of buforin IIb.

2. Materials and methods

2.1. Peptides

Buforin IIb (RAGLQFPVG[RLLR]$_3$), BUF(1–17) (TRSSRAGLQFPVGRVHR), and magainin G (GIGKFLHSAKKFAKAFVAEIMNS) were synthesized on a MilliGen 9050 peptide synthesizer. Synthetic peptides were purified by RP-HPLC and characterized by mass spectroscopy and amino acid analysis. Biotinylation and FITC-labeling of peptides were performed with Biotin-NHS and FITC Labeling Kit (Calbiochem, SD, CA), respectively, according to the manufacturer's protocol. The biotinylated- and FITC-labeled peptides had the same cytotoxic activity against HeLa and Jurkat cells as the parent peptide, which indicated that biotinylation and FITC-labeling had no adverse effects on the cytotoxic activity of the peptides (data not shown).

2.2. In vitro cytotoxicity assay

Cells were cultured in 96-well plates (10^4 cells/well) in a complete medium [Dulbecco's modified eagle medium (DMEM) with 10% FBS for HeLa cells, human fibroblasts, and mouse embryonic fibroblasts, and RPMI 1640 with 10% FBS for Jurkat cells and peripheral blood lymphocytes]. After 24 h of incubation, cells were treated with peptides (0–200 μg/ml) and incubated for another 48 h. Cell viability was measured with the 3-(4,5-dimethylthiazol-2-yl)-2,5-diphenyl tetrazolium bromide (MTT) assay using the CellTiter 96-cell proliferation assay kit (Promega, Madison, WI), and the IC_{50} value was calculated as the concentration of peptide that induced 50% growth inhibition compared to a untreated control. In addition, the anticancer activity that buforin IIb displayed against 60 human tumor cell lines was determined as part of the Developmental Therapeutics Program of the United States National Cancer Institute (NCI).

2.3. FACS analysis and confocal fluorescence microscopy

Jurkat cells (10^5) were incubated with peptides (40 μg/ml) for 30 min. To determine intracellular K^+ levels, the cells were loaded with cell-permeant potassium-binding benzofuran isophthalate-AM (PBFI-AM, 5 μM; Molecular Probes, Eugene, OR) for 30 min, and 10^4 cells per sample were analyzed by flow cytometry (FACSVantage SE, Becton–Dickinson, Franklin Lakes, NJ) [9]. To determine the subcellular location of the peptides, HeLa cells or human fibroblasts (2×10^5) were plated on a glass coverslip, grown overnight, and then incubated with biotin-labeled peptides (20 μg/ml for HeLa and 80 μg/ml for human fibroblasts). After 24 h of incubation, the cells were rinsed twice with PBS for the observation of the living cells. For the fixed cells, the protocol was the same, but, in addition, they were fixed and permeabilized by incubation with 4% paraformaldehyde in 0.2% Triton X-100 for 30 min. Biotin-labeled peptides were visualized with 2 μg/ml of FITC-streptavidin (Roche, Mannheim, Germany) and observed with a Carl Zeiss LSM 410 confocal microscope (Jena, Germany).

2.4. Interaction between buforin IIb and cell surface components

To examine the interaction between buforin IIb and cell surface components, competitive-binding assays were performed. Briefly, cells were treated with gangliosides (monosialoganglilside GM_3 from canine blood), heparins, or phosphatidylserines (0–50 μg/ml, Sigma, St. Louis, MO) in the presence of peptides (at IC_{50}). After 48 h of incubation, cell viability was measured with the MTT assay, and % viability was examined relative to untreated cells. To further confirm the identity of the buforin IIb-binding site on the cell surface, ganglioside- or sialic acid-depleted cells were prepared for cell viability assay. For the deletion of ganglioside, cells were treated with 0–5 μM 1-phenyl-2-palmitoylamino-3-morpholino-1-propanol (PPMP, Sigma) and grown for 2 days. Alternatively, sialic acids were removed by a 1-h incubation of cells with sialidase (0–50 units/ml, NEB, Ipswich, MA). Cell viability was examined after a 48-h incubation of these cells with buforin IIb as described above.

2.5. Uptake of buforin IIb into cells

Jurkat cells (10^5) were treated with FITC-labeled buforin IIb (0–6 μg/ml) for 2 h, and the cellular uptake of buforin IIb was determined by flow cytometry. To determine the effects of gangliosides on the uptake of buforin IIb, Jurkat cells were also incubated with FITC-labeled buforin IIb (6 μg/ml) in the presence of gangliosides (0–20 μg/ml), or pretreated with 5 μM PPMP.

2.6. Detection of apoptosis

To detect apoptosis, Jurkat cells (2×10^5) were incubated with PBS, buforin IIb (20 μg/ml), or etoposide (10 μM) for 24 h, and cells that were undergoing apoptosis were identified by staining with annexin V-FITC (150 ng/ml) and propidium iodide (PI, 1 μM, Sigma). 10^4 cells per sample were analyzed by flow cytometry. For the detection of DNA fragmentation induced by apoptosis, Jurkat cells were treated with PBS, buforin IIb, or staurosporine (1 μM, Sigma). DNA was extracted, electrophoresed on a 1.5% agarose gel, and visualized under UV illumination. In addition, Western blot analysis of HeLa cells treated with buforin IIb was performed using anti-caspase-9, anti-caspase-3, anti-poly (ADP-ribose) polymerase (PARP, Cell Signaling Tech., Danvers, MA), and anti-actin antibodies (Sigma).

2.7. In vivo antitumor efficacy of buforin IIb in tumor xenografts

NCI-H460 cells (2×10^6), which were derived from a patient with large cell lung cancer, resus-

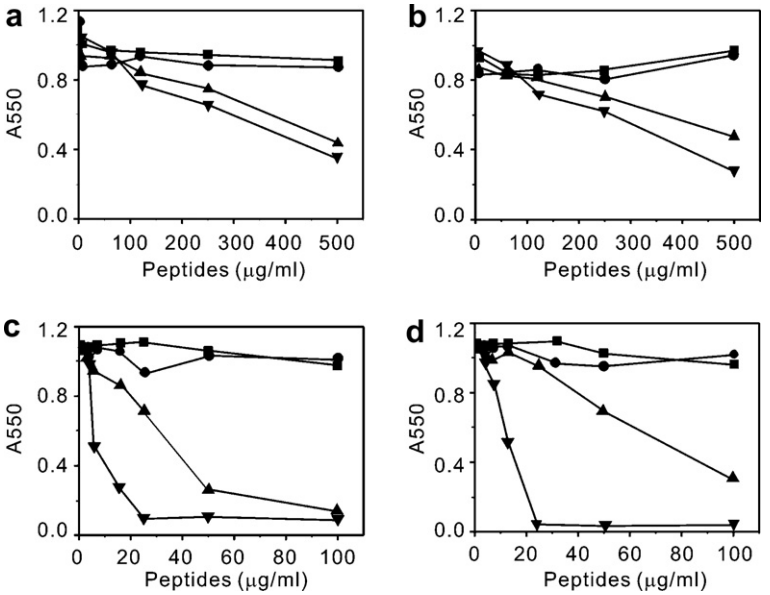

Fig. 1. *In vitro* cytotoxicity of buforin IIb. Buforin IIb (▼), BUF(1–17) (●), magainin G (▲), or PBS (■) was added to human fibroblasts (a), mouse embryonic fibroblasts (b), Jurkat cells (c), and HeLa cells (d). After a 48-h incubation with the peptides, cell viability was measured by the MTT assay. Data represent the mean of duplicate samples from 1 of 2 similar experiments.

pended in 0.1 ml of DMEM were transplanted subcutaneously in the hindlimb regions of BALB/c (*nu/nu*) mice. At the onset of palpable tumor (volume: ~150 mm^3), mice were randomly divided into 4 groups, whereby one group ($n = 6$) was injected intravenously with 20 mg/kg buforin IIb, a second group with 10 mg/kg, a third group with 5 mg/kg, and the fourth control group with equivalent volumes of PBS on days 1, 2, 4, and 8. Tumor measurements were done every 4 days and the tumor volume (mm^3) was calculated as length × $width^2$ × 0.5.

3. Results

3.1. Anticancer activity of buforin IIb

We found that buforin IIb was cytotoxic to cancer cells but not to normal proliferating cells. For cancer cells, buforin IIb showed IC_{50} values of 6 μg/ml for Jurkat and 12 μg/ml for HeLa cells, whereas for normal cells, such as human fibroblasts, mouse embryonic fibroblasts and peripheral blood lymphocytes, the IC_{50} for buforin IIb was about 350 μg/ml (Fig. 1 and data not shown). Buforin IIb was much more toxic to cancer cells than the well-characterized peptide magainin G ($IC_{50} = 34$–68 μg/ml), and a buforin II truncated analog, BUF(1–17), did not display robust anticancer activity ($IC_{50} > 500$ μg/ml). In the human tumor cell line testing program (http://dtp.nci.nih.gov/branches/btb/ivclsp.html), buforin IIb displayed potent cytotoxic activity against all 60 different types of human tumor cells ($IC_{50} = 7.2$–23.9 μg/ml), suggesting that the mechanism of buforin IIb cytotoxicity is the same in all tumor cells (Table 1). These finding imply that the molecular target(s) of buforin IIb is universally present in cancer cell.

3.2. Mechanism of an anticancer action

The interaction of buforin IIb with Jurkat cell membranes was studied by measuring intracellular K^+ levels using PBFI-AM. Buforin IIb-treated cells displayed the same fluorescence as the untreated cells upon loading with PBFI-AM (Fig. 2a), suggesting that the integrity of the cell is maintained in buforin IIb-treated cells. On the other hand, cells treated with magainin G showed two populations, one with normal potassium-related fluorescence and the other with lower fluorescence compared to the untreated cells, implying the involvement of an intracellular K^+ efflux. Moreover, confocal microscopic images

Table 1
Antitumor activity of buforin IIb against 60 human tumor cell lines*

Cell lines	IC_{50} (μg/ml)	Cell lines	IC_{50} (μg/ml)	Cell lines	IC_{50} (μg/ml)
Leukemia		CNS cancer		Ovarian cancer	
CCRF-CEM	14.7	SF-268	12.4	IGROV1	9.0
HL-60	11.3	SF-295	12.9	OVRCAR-3	15.2
K-562	8.2	SF-539	9.5	OVRCAR-4	17.6
MOLT-4	17.0	SNB-19	13.8	OVRCAR-5	13.8
RPMI-8226	10.5	SNB-75	15.5	OVRCAR-8	13.0
SR	20.2	U251	10.6	SK-OV-3	12.6
Breast cancer		Melanoma		Colon cancer	
MCF7	15.1	LOX IMVI	9.5	COLO 205	11.2
NCI/ADR-RES	11.5	MALME-3M	10.9	HCT-116	14.6
MDA-MB-231	11.3	M14	15.1	HCT-15	13.2
HS 578T	11.7	SK-MEL-2	11.1	HT29	17.6
MDA-MB-435	11.3	SK-MEL-5	8.9	KM12	12.0
MDA-N	10.6	UACC-257	12.5	SW-620	12.7
BT-549	12.9	UACC-62	10.6		
T-47D	23.9				
Non-small cell lung cancer		Renal cancer		Prostate cancer	
A549	11.7	786-0	12.2	PC-3	12.0
EKVX	12.1	A498	10.0	DU-145	15.3
HOP-62	12.6	ACHN	12.0		
HOP-92	7.2	CAKI-1	14.1		
NCI-H226	13.3	RFX 393	11.0		
NCI-H23	10.8	SN12C	11.4		
NCI-H322M	10.7	TK-10	13.1		
NCI-H460	12.1	UO-31	10.6		
NCI-H522	11.2				

* Data from the NCI testing program.

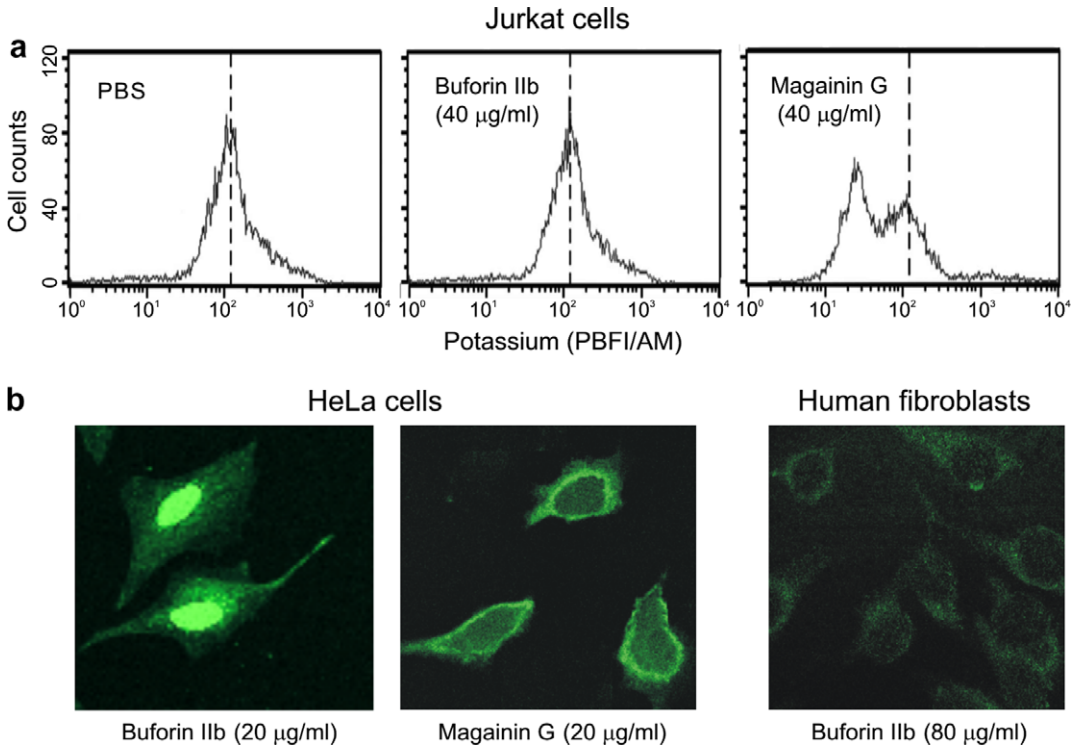

Fig. 2. FACS analyses and confocal fluorescence microscopic images. (a) FACS analyses. Jurkat cells were incubated with PBS, buforin IIb, or magainin G for 30 min, followed by the addition of PBFI-AM. 10^4 cells were analyzed by flow cytometry. (b) Confocal fluorescence microscopic images. HeLa cells were treated with biotin-labeled buforin IIb or magainin G, and human fibroblasts were treated with biotin-labeled buforin IIb. After fixation, the cells were visualized with streptavidin-FITC.

revealed that biotin-labeled buforin IIb penetrated the HeLa cell membrane and accumulated primarily in the nuclei (Fig. 2b). In contrast, biotin-labeled magainin G associated with the membrane. These results indicate that, unlike membrane-acting peptides such as magainin G [5], buforin IIb proceeds through membranes without disrupting them and the eventual molecular target of buforin IIb in cancer cells is an intracellular molecule, not the membranes. Buforin IIb did not penetrate normal cells (human fibroblasts, mouse embryonic fibroblasts, and peripheral blood lymphocytes) even at a concentration of 80 μg/ml (Fig. 2b and data not shown). The intracellular distribution of buforin IIb in HeLa cells was not altered by the fixation process (Fig. S1).

3.3. Buforin IIb requires cell surface gangliosides for internalization

To identify the binding-targets on the cell membranes for internalization of buforin IIb into cancer cells, we examined whether exogenous gangliosides, heparins, or phosphatidylserines affect the ability of buforin IIb to enter cancer cells and kill them. As shown in Fig. 3a, the % viability of buforin IIb-treated cancer cells increased with increasing concentrations of gangliosides in the medium, implying that exogenous gangliosides prevent buforin IIb from penetrating cancer cells. The addition of exogenous heparins and phosphatidylserines had less of an effect on the viability of cancer cells in the presence of buforin IIb (Fig. 3b, c). When treated alone, gangliosides, heparins, or phosphatidylserines did not affect cell viability at concentrations up to 50 μg/ml (data not shown). The inhibition of buforin IIb entry by exogenous gangliosides was confirmed by flow cytometry. In a dose-response experiment with FITC-labeled buforin IIb, the fluorescence intensity of buforin IIb-treated cells enhanced with increasing concentrations of buforin IIb (Fig. 3d). However, in the presence of exogenous gangliosides, the fluorescence intensities of cells treated with the same concentration of buforin IIb decreased significantly relative to the corresponding minus-ganglioside control (Fig. 3e).

To confirm the role of gangliosides in the binding and uptake of buforin IIb, we analyzed cancer cells that had been treated with PPMP, an inhibitor of ganglioside synthesis. When PPMP-treated Jurkat cells and PPMP-untreated cells were incubated with the same amount of FITC-labeled buforin IIb, the fluorescence intensities of

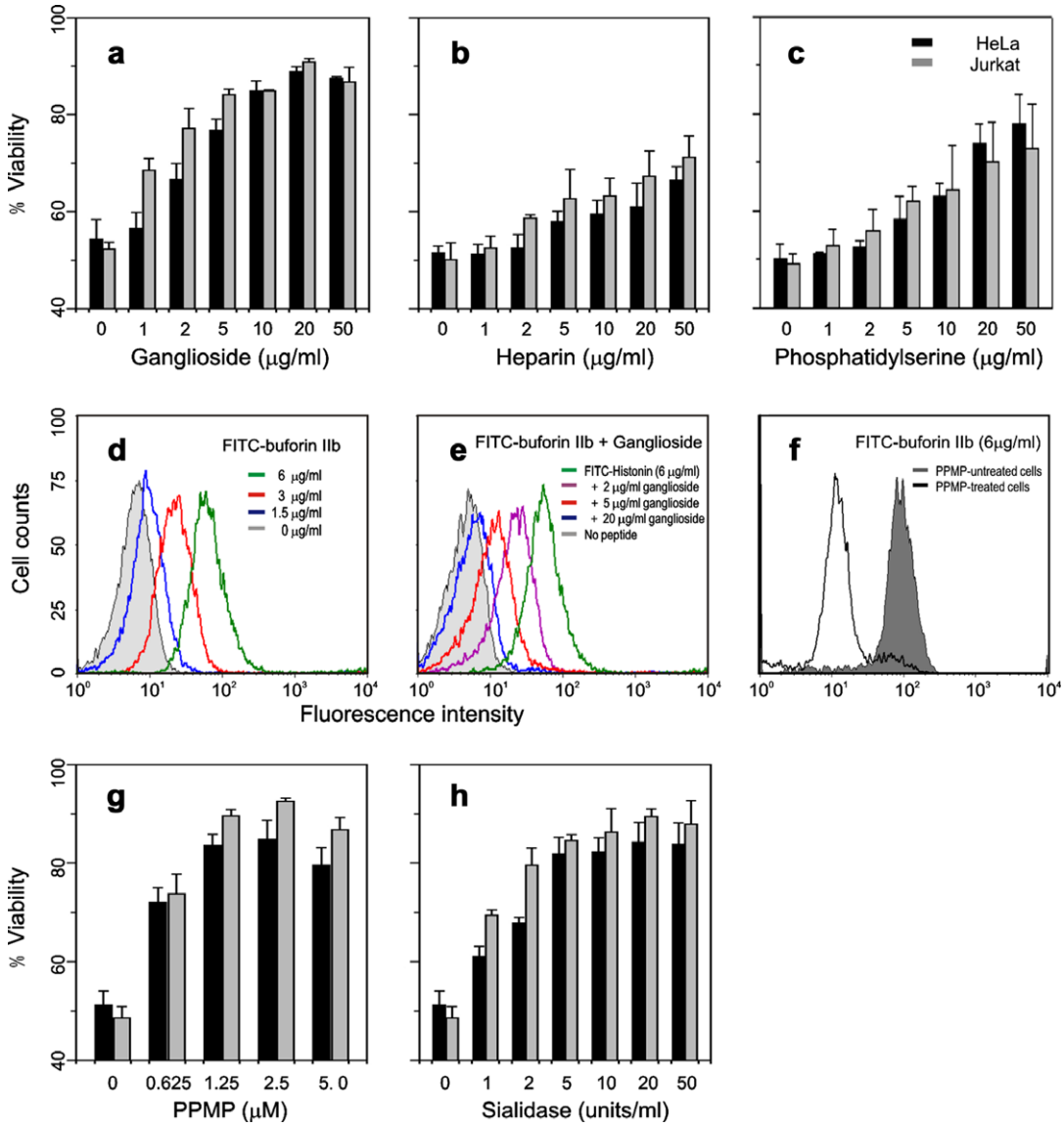

Fig. 3. Cell viability and FACS analyses of cancer cells treated with buforin IIb. (a–c) Effects of gangliosides, heparins, and phosphatidylserines on cell viability. Viability of HeLa (black bars) and Jurkat (gray bars) cells treated with buforin IIb in the presence of various concentrations of gangliosides (a), heparins (b), or phosphatidylserines (c), as determined by the MTT assay. (d–f) Uptake of buforin IIb. Jurkat cells were treated with various concentrations of FITC-labeled buforin IIb only (c) or with FITC-labeled buforin IIb in the presence of various concentrations of gangliosides (d). In (f), Jurkat cells were pretreated with 5 μM PPMP for gangliosides depletion. Cellular uptake of buforin IIb was determined by flow cytometry. (g,h) The influence of gangliosides or sialic acid depletion on cell viability. After treatment with PPMP (e) or sialidase (f), viability of cells exposed to buforin IIb was determined by the MTT assay. Data in (a), (b), (c), (g), and (h) represent the mean ±SD of 3 independent experiments.

PPMP-treated cells were significantly lower than the corresponding PPMP-untreated control (Fig. 3f). Moreover, the PPMP-treated HeLa and Jurkat cells showed 85% and 93% viability, respectively, as compared to 50% viability for the PPMP-untreated cells (Fig. 3g). We also examined whether or not the depletion of sialic acids on the cell surface affected buforin IIb cytotoxicity. As shown in Fig. 3h, the sialic acid-depleted HeLa and Jurkat cells displayed 85% and 90% viability, respectively, whereas the sialic acid non-depleted cells displayed only 50% viability. When treated alone, neither PPMP (5 μM) nor sialidase (50 units/ml) affected cell viability

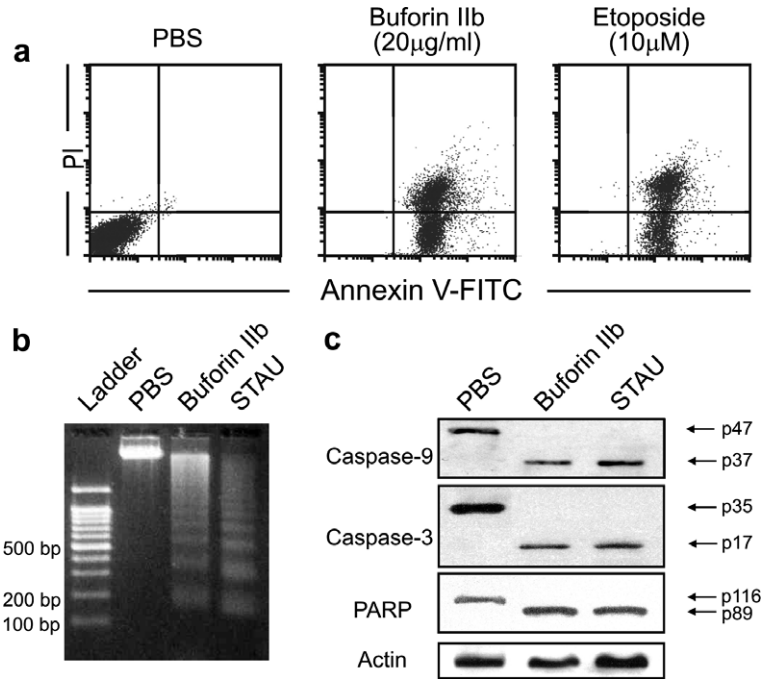

Fig. 4. Induction of apoptosis in cancer cells treated with buforin IIb. (a) FACS analyses of Jurkat cells treated with PBS, buforin IIb, or etoposide by staining with annexin V-FITC/PI. (b) Detection of DNA fragmentation in Jurkat cells treated with PBS, buforin IIb, or staurosporine (STAU, 5 μM). For comparison, the first lane shows a DNA ladder created by Promega. (c) Western blot analyses of caspases and PARP in HeLa cells treated with PBS, buforin IIb or staurosporine. The molecular sizes of the proteins are indicated with arrows at the right. Actin is shown as a control.

(data not shown). Overall, these results suggest that cell surface gangliosides or sialic acids are important for buforin IIb-entry into cancer cells.

3.4. Buforin IIb induces apoptosis

We next sought to determine the mode by which buforin IIb kills cancer cells by examining buforin IIb-induced apoptosis. Apoptosis of Jurkat cells was detected by annexin V-FITC/PI staining and DNA laddering. FACS analyses revealed that 50% of the cells were in the early apoptotic stage (annexin V-FITC single staining), and 50% were in the late apoptotic stage (annexin V-FITC/PI double staining) (Fig. 4a). As shown in Fig. 4b, chromosomal DNA from the buforin IIb-treated cells was fragmented into nucleosomal ladders. The data clearly indicate that buforin IIb induces apoptosis of cancer cells. The buforin IIb-induced apoptotic pathway was further investigated by Western blot analysis of caspases, which are key effectors of apoptosis. Buforin IIb induced the activation of pro-caspase-9 (a caspase that initiates mitochondria-dependent apoptosis) and pro-caspase-3 (a key mediator of apoptosis of mammalian cells). Caspase-3 activity was measured using the caspase-3 substrate PARP (Fig. 4c). The cleavage of PARP observed in buforin IIb-treated cells was identical to that observed in staurosporine-treated cells. The activation of these apoptotic pathways suggests that buforin IIb causes cell death by inducing mitochondria-dependent apoptosis. Mitochon-

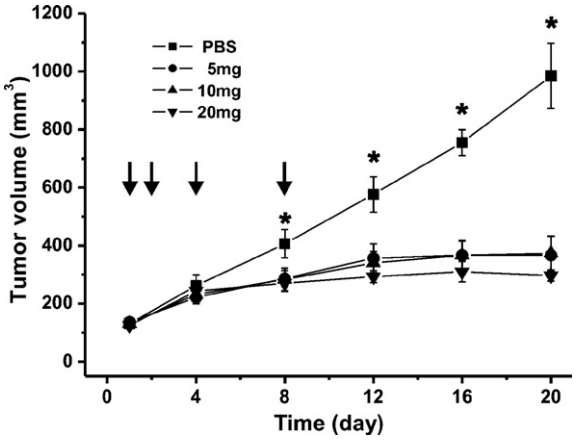

Fig. 5. *In vivo* tumor suppressing activity of buforin IIb in mouse tumor xenografts. NCI-H460 cells were transplanted to BALB/c (*nu/nu*) mice in the hindlimb regions. Administration was started on day 1 when the tumor volume reached approximately 150 mm^3. 5 mg/kg (●), 10 mg/kg (▲), and 20 mg/kg (▼) of buforin IIb or PBS (■) was administrated by intravenous injection at the time indicated by arrows. Data are expressed as tumor volume (mm^3). *Bars*, SEs ($n = 6$). $^*P < 0.05$ as determined by Student's *t* test.

dria-dependent apoptosis in the presence of buforin IIb was further confirmed by Western blot analysis, which showed release of cytochrome *c*, a mitochondrial protein, into the cytosolic fraction of the buforin IIb-treated HeLa cells (data not shown).

3.5. Buforin IIb is efficacious in tumor xenografts

The *in vivo* activity of buforin IIb was tested against NCI-H460 implanted into mice. Buforin IIb displayed remarkable suppression of tumor xenografts at concentrations of more than 5 mg/kg (Fig. 5). Comparison of mean tumor volumes in controls and buforin IIb-treated mice using a Student's *t* test revealed a significant difference ($P < 0.05$) beginning on day 8 through study completion.

4. Discussion

In this study, we have demonstrated that buforin IIb, a potent, cell-penetrating AMP derived from histone H2A, selectively kills cancer cells. The remarkable selectivity of buforin IIb for cancer cells results largely from the inability of the peptide to penetrate normal cell membranes. Cationic AMPs display selective toxicity toward bacteria, and negatively charged phospholipids and polyanionic lipopolysaccharides are abundant on the surfaces of bacterial membranes [10]. Similarly, the surfaces of the plasma membranes of cancer cells contain a high concentration of negatively charged gangliosides (see below). In contrast, the impenetrable surface of normal mammalian cell membranes is mainly composed of neutral zwitterionic phospholipids and sterols [11]. Many researchers report that negatively charged gangliosides are abundant in the outer surface of cancer cell membranes [12,13]. Thus we examined whether the cytotoxicity of buforin IIb is affected by exogenously added gangliosides. These competitive-binding assays, described herein, clearly demonstrate that gangliosides on the surfaces of cancer cells function as target molecules for buforin IIb binding. This observation is further supported by the findings that cell lines with PPMP-induced ganglioside depletion fail to internalize buforin IIb, and the treatment of cells with sialidase blocks the buforin IIb internalization. In addition to gangliosides, other negatively charged components found on the surfaces of cancer cells, such as phosphatidylserine (PS) and heparan sulfate (HS), might also represent potential targets for buforin IIb binding. Papo et al. recently reported that the host defense-like peptide D-K_6L_9 selectively targets cancer cells by binding to surface-exposed phosphatidylserine [14], However, our experiments showed that heparin, a structural homolog of HS, and phosphatidylserine have little effect on the binding of buforin IIb to cancer cells. Our data clearly show that gangliosides on the surfaces of cancer cells are specific binding sites for buforin IIb and that it is these molecules that allow buforin IIb to distinguish cancer cells from normal cells.

After specifically targeting cancer cells through interaction with gangliosides, buforin IIb induces apoptosis in cancer cells by a mitochondria-dependent pathway, as confirmed by caspase-9 activation and cytochrome *c* release to cytosol as well as by DNA laddering and annexin V staining (Fig. 4). Mitochondria-dependent apoptosis has also been observed with other synthetic anticancer peptides, such as RGD-tachyplesin [15] and DP1 [16], which consist of a tumor-targeting peptide and an AMP. Although the precise mechanism is not known, these peptides were reported to induce apoptosis by disrupting mitochondrial membranes. Ongoing studies are aimed at investigating the precise mechanism of buforin IIb-mediated apoptosis.

In conclusion, our results clearly demonstrate that, because of selective cell membrane penetration and subsequent induction of apoptosis, buforin IIb displays strong, selective anticancer activity against a broad spectrum of cancer cells. Moreover, *in vivo* analysis of buforin IIb revealed that it displayed significant tumor suppression activity in mice with tumor xenograft. Our findings may help to promote the design of novel therapeutic drugs for the treatment of cancers.

Conflict of interest

We declare that we do not have any financial and personal relationship with other people or organizations that could inappropriately influence (bias) our work.

Acknowledgements

This work was supported by grants from the 21C Frontier Program of Microbial Genomics and Applications (MG05-0204-1-0) and Molecular and Cellular BioDiscovery Research Program (M1-0106-00-0200) from the Ministry of Science and Technology of Korea, and by Grants from the Basic

Research Program of the Korea Science and Engineering Foundation (R01-2005-000-11010-0) and the Korea Research Foundation (KRF-2004-042-D00072).

Appendix A. Supplementary data

Supplementary data associated with this article can be found, in the online version, at doi:10.1016/j.canlet.2008.05.041.

References

[1] R. ez-Tomás, Multidrug resistance: retrospect and prospects in anti-cancer drug treatment, Curr. Med. Chem. 13 (2006) 1859–1876.
[2] N. Papo, Y. Shai, Host defense peptides as new weapons in cancer treatment, Cell Mol. Life Sci. 62 (2005) 784–790.
[3] S.V. Sharma, Melittin resistance: a counterselection for ras transformation, Oncogene 7 (1992) 193–201.
[4] A.J. Moore, D.A. Devine, M.C. Bibby, Preliminary experimental anticancer activity of cecropins, Pept. Res. 7 (1994) 265–269.
[5] R.A. Cruciani, J.L. Barker, M. Zasloff, H.C. Chen, O. Colamonici, Antibiotic magainins exert cytolytic activity against transformed cell lines through channel formation, Proc. Natl. Acad. Sci. USA 88 (1991) 3792–3796.
[6] G.S. Yi, C.B. Park, S.C. Kim, C. Cheong, Solution structure of an antimicrobial peptide buforin II, FEBS Lett. 398 (1996) 87–90.
[7] C.B. Park, H.S. Kim, S.C. Kim, Mechanism of action of the antimicrobial peptide buforin II: buforin II kills microorganisms by penetrating the cell membrane and inhibiting cellular functions, Biochem. Biophys. Res. Commun. 244 (1998) 253–257.
[8] C.B. Park, K.S. Yi, K. Matsuzaki, M.S. Kim, S.C. Kim, Structure-activity analysis of buforin II, a histone H2A-derived antimicrobial peptide: the proline hinge is responsible for the cell-penetrating ability of buforin II, Proc. Natl. Acad. Sci. USA 97 (2000) 8245–8250.
[9] B. Dallaporta, T. Hirsch, S.A. Susin, N. Zamzami, N. Larochette, C. Brenner, I. Marzo, G. Kroemer, Potassium leakage during the apoptotic degradation phase, J. Immunol. 160 (1998) 5605–5615.
[10] R.E. Hancock, H.G. Sahl, Antimicrobial and host-defense peptides as new anti-infective therapeutic strategies, Nat. Biotechnol. 24 (2006) 1551–1557.
[11] R.I. Lehrer, A.K. Lichtenstein, T. Ganz, Defensins: antimicrobial and cytotoxic peptides of mammalian cells, Annu. Rev. Immunol. 11 (1993) 105–128.
[12] N. Hanai, K. Nakamura, K. Shitara, Recombinant antibodies against ganglioside expressed on tumor cells, Cancer Chemother. Pharmacol. 46 (2000) S13–17.
[13] R.J. Bitton, M.D. Guthmann, M.R. Gabri, A.J. Carnero, D.F. Alonso, L. Fainboim, D.E. Gomez, Cancer vaccines: an update with special focus on ganglioside antigens, Oncol. Rep. 9 (2002) 267–276.
[14] N. Papo, D. Seger, A. Makovitzki, V. Kalchenko, Z. Eshhar, H. Degani, Y. Shai, Inhibition of tumor growth and elimination of multiple metastases in human prostate and breast xenografts by systemic inoculation of a host defense-like lytic peptide, Cancer Res. 66 (2006) 5371–5378.
[15] Y. Chen, X. Xu, S. Hong, J. Chen, N. Liu, C.B. Underhill, K. Creswell, L. Zhang, RGD-Tachyplesin inhibits tumor growth, Cancer Res. 61 (2001) 2434–2438.
[16] J.C. Mai, Z. Mi, S.H. Kim, B. Ng, P.D. Robbins, A proapoptotic peptide for the treatment of solid tumors, Cancer Res. 61 (2001) 7709–7712.